



Research Interests and Selected Recent Publications.

Theory, modeling, and simulation of processes on surfaces.

My research work is related to the following lines:

- (1) Low-Energy Electron Diffraction (LEED). I work on the theory and methodology of this technique, and analyzing experiments on actual surfaces
- (2) Ab-initio modeling of adsorption and diffusion of molecules on surfaces. Calculations of vibrational and optical properties of surfaces. Molecular dynamics. Physical-chemistry.
- (3) Ballistic Emission Electron Microscopy (BEEM).

I have been working recently with the following materials:

- (1) Substrates: Pt, Pd, Ni, Cu, Al, Fe, TiO₂, C (graphene), etc.
- (2) Adsorbates: H, O, C, O₂, O₃, C₆H₆, CO, CO₂, H₂O, etc.

A few selected recent publications follow:

Structure of Rutile TiO_2 $(110)-(1 \times 2)$: Formation of Ti_2O_3 Quasi-1D Metallic Chains

M. Blanco-Rey, J. Abad, C. Rogero, J. Mendez, M. F. Lopez, J. A. Martin-Gago, and P. L. de Andres

Instituto de Ciencia de Materiales (CSIC), Cantoblanco, 28049 Madrid, Spain

(Received 8 November 2005; published 6 February 2006)

Combining STM, LEED, and density functional theory, we determine the atomic surface structure of rutile TiO_2 $(110)-(1 \times 2)$: nonstoichiometric Ti_2O_3 stripes along the $[001]$ direction. LEED patterns are sharp and free of streaks, while STM images show monatomic steps, wide terraces, and no cross-links. At room temperature, atoms in the Ti_2O_3 group have large amplitudes of vibration. The long quasi-1D chains display metallic character, show no interaction between them, and cannot couple to bulk or surface states in the gap region, forming good atomic wires.

DOI: 10.1103/PhysRevLett.96.055502

PACS numbers: 68.35.Bs, 61.14.Hg, 68.47.Gh, 73.90.+f

A better understanding of metal oxide surfaces will certainly make a huge impact on technologically important fields like heterogeneous catalysis, photochemistry, gas sensing, anticorrosion coatings, etc. [1]. Metal oxides, and in particular TiO_2 , are the most extensively used support in catalytic devices. To design new catalysts, or to improve existing ones, a full description of their structural and electronic properties is necessary. The (110) face of TiO_2 makes a paradigmatic example as its most stable face and is known to host interesting surface chemistry. However, only recently has the geometrical disposition of atoms on the 1×1 surface been quantitatively determined by full dynamical low-energy electron diffraction (LEED) work [2]. Upon annealing, this face is reduced and results in a 1×2 reconstruction. Several models for this reconstruction have been proposed to explain qualitatively the STM images [Fig. 2(b) below], but these models have differed even on the surface stoichiometry, e.g., (i) Ti_2O_3 “added row” [3], (ii) “missing row” [4], (iii) “missing unit” [5], etc. In this work, we combine scanning tunneling microscopy (STM), full dynamical LEED, and density functional theory (DFT) to get a quantitative structural determination of the 1×2 reconstruction on (110) rutile TiO_2 . The structure shows the existence of long nonstoichiometric Ti_2O_3 added rows, in agreement with Onishi’s model [3] (Fig. 1). The chemisorption energy for one of those Ti_2O_3 groups is 5.4 eV per unit cell, very similar to the bonding interaction between Ti_2O_3 and TiO_2 (6.3 eV), and it is useful to visualize the group as an adsorbed molecule producing long quasi-one-dimensional strips on the surface (Fig. 2). Most interesting, these quasi-1D molecular wires have a metallic character, making an ideal system to carry experiments to study 1D conductance. The outer oxygen on the Ti_2O_3 group [labeled O(1) in Fig. 1] have an unusual large rms vibration amplitude (about 0.36 Å), related to a relatively flat potential region around these positions. It is worth noticing the buckling in the trough: Ti(d) and O(5) are separated by a vertical distance of 0.46 Å. Finally, while typical Ti-Ti distances in bulk are 3.56 Å, we find that both Ti(b) and Ti(c) are attracted to Ti(a), to distances of 3.36 and 3.44 Å.

Experiments have been performed at room temperature on a TiO_2 rutile single crystal (PI-KEM Ltd., UK), treated by cycles for Ar^+ ion bombardment (1 keV, 10–30 min) under ultrahigh vacuum conditions (base pressure 2×10^{-10} mbar). The absence of contaminants has been judged by Auger electron spectroscopy. Annealing conditions have been carefully investigated to get a well characterized reconstruction (1150 K, 60 min). This procedure gives a very sharp 1×2 LEED pattern, with low background. STM images were recorded *in situ* at constant current mode and room temperature. Tungsten tips were prepared by field emission. Prolonged electron beam exposure during the LEED $I(V)$ measurements produces degradation of the LEED spots and increasing background intensity. To avoid these effects, the sample was displaced at short time intervals to expose fresh areas to the electron beam, and the sample was reannealed (1150 K, 10–30 min) to restore the 1×2 pattern to the initial quality. $I(V)$ curves have been measured at normal and off-normal incidence to increase the accuracy of the structural analysis. Figure 2(a) shows a STM representative image. We

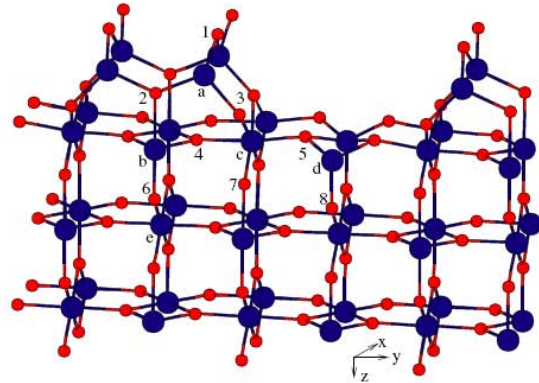


FIG. 1 (color online). Model for 1×2 TiO_2 (110) (best fit to LEED, $R_p = 0.28$). Large and small spheres represent Ti(a–e) and O(1–8) atoms, respectively. The lowest layer has been frozen to optimized bulklike positions.

LEED-IV study of the rutile $\text{TiO}_2(110)\text{-}1\times 2$ surface with a Ti-interstitial added-row reconstruction

M. Blanco-Rey,^{1,*} J. Abad,² C. Rogero,³ J. Méndez,¹ M. F. López,¹ E. Román,¹ J. A. Martín-Gago,¹ and P. L. de Andrés¹

¹*Instituto de Ciencia de Materiales (CSIC), Cantoblanco, 28049 Madrid, Spain*

²*Centro de Investigación en Óptica y Nanofísica, Universidad de Murcia, Campus Espinardo, 30100 Murcia, Spain*

³*Centro de Astrobiología (CSIC-INTA), Carretera de Ajalvir km. 4, 28850 Torrejón de Ardoz, Madrid, Spain*

(Received 22 November 2006; revised manuscript received 22 December 2006; published 9 February 2007)

Upon sputtering and annealing in UHV at ~ 1000 K, the rutile $\text{TiO}_2(110)$ surface undergoes a $1\times 1 \rightarrow 1\times 2$ phase transition. The resulting 1×2 surface is Ti rich, formed by strands of double Ti rows as seen on scanning tunneling microscopic images, but its detailed structure and composition have been subject to debate in the literature for years. Recently, Park *et al.* [Phys. Rev. Lett. **96**, 226105 (2006)] have proposed a model where Ti atoms are located on interstitial sites with Ti_2O stoichiometry. This model, when it is analyzed using LEED-IV data [Phys. Rev. Lett. **96**, 0055502 (2006)], does not yield an agreement between theory and experiment as good as the previous best fit for Onishi and Iwasawa's model for the long-range 1×2 reconstruction. Therefore, the Ti_2O_3 added row is the preferred one from the point of view low-energy electron diffraction.

DOI: 10.1103/PhysRevB.75.081402

PACS number(s): 61.14.Hg, 68.35.Bs, 68.47.Gh

Metal oxide surfaces are a subject of strategic interest due to their wide range of technological applications. They are popular as a support for heterogeneous catalysis, but are also highly appreciated for their use in photocatalysis, anticorrosion coatings, pigments, gas sensing, biocompatibility, environmental applications, etc.¹ Among the different rutile surfaces, $\text{TiO}_2(110)$ is the most popular due to its stability and favorable morphology, and it is considered in the literature as a benchmark for modeling the structure and electronic properties of metal oxides. The bulk rutile is characterized by rows of alternatively oriented oxygen octahedra centered at titanium atoms. The $\{110\}$ cut produces a relatively flat surface; however, only recently has a structural determination by low-energy electron diffraction (LEED) been considered accurate enough to bring wide consensus to the quantitative values for the different atomic positions.² Most interesting, moreover, is the 1×2 reconstruction that appears on the clean surface upon annealing up to ~ 1000 K in ultrahigh vacuum (UHV). From scanning tunneling microscopy (STM) it has been well established that this phase consists of long stripes running along the $[001]$ crystallographic direction. By careful formation of this new stable phase, these chains can be formed nearly without interruption on the typical distances of terraces—i.e., 100–1000 Å long. These chains are known to depart from the surface stoichiometry and are usually characterized as a reduced Ti rich 1×2 reconstruction.³ From a combined approach using STM, LEED and density functional theory (DFT), recently we predicted that these stripes may possess interesting quasi-one-dimensional properties.⁴ The complexity of the reconstruction, however, is enough to allow for many different geometrical configurations; even a possible reversible transformation between the 1×1 and the 1×2 phases has been reported,⁵ not to mention the existence of *cross-links* between chains with an entirely different stoichiometry or other defects on the surface.⁶ Some of these phenomena might well depend on the careful conditions to recreate the 1×2 reconstruction, and the fact is that this system is a challenge

for both theory and experiment. Therefore, it is important to realize that the formation of a 1×2 phase may certainly be influenced by external parameters (e.g., UHV or not, the particular ambience if any, different temperatures and times for annealing, etc). The geometrical structure of the 1×2 phase has been much studied in the literature by STM, but these experiments cannot give a clear description of the atomic positions or even the surface stoichiometry. Hence, different proposals can be found in the literature: (i) a missing-row model⁷ where bridging oxygen atoms are desorbed into vacuum in competition with diffusion of bulk lattice oxygen atoms moving to the surface, (ii) an added-row model with a Ti_2O_3 stoichiometry³ where the Ti cations move to octahedral sites and oxygen atoms stay near their bulklike positions, (iii) an added-row model with a Ti_3O_5 stoichiometry⁸ where all the atoms remain near their bulk positions, and (iv) a stoichiometric model⁶ where the added rows proposed by Pang *et al.* have been modified by adding oxygen to create an added row of Ti_3O_6 .

LEED is known to be very sensitive to the final disposition of the atoms on the surface. However, by analyzing only the Bragg spots, we obtain information about the ordered long-range structures. To study the geometry of disordered short-range structures, defects, etc. one should focus on the diffuse LEED intensities measured at low-temperatures, which is beyond our experimental setup. We have used LEED-IV for the 1×2 reconstruction to test all these different models against full multiple-scattering calculations.⁴ An objective quantitative comparison between experimental and theoretical LEED-IV curves can be obtained by computing a suitable R factor that can be used to identify relevant best-fit models. We have used Pendry's R factor,⁹ a widely accepted relevant and accurate number to characterize real structures.¹⁰ Pendry's R factor R_P takes values between 0 and 2; values below 0.3 yield a reasonable good correlation between theory and experiment, while values over 0.5 mark the onset of spurious chaotic correlations.¹¹

Recently, a new structural candidate for the 1×2 recon-

Strong covalent bonding between two graphene layers

P. L. de Andres, R. Ramírez, and J. A. Vergés

Instituto de Ciencia de Materiales de Madrid (CSIC), Cantoblanco, 28049 Madrid, Spain

(Received 24 September 2007; published 2 January 2008)

We show that two graphene layers stacked directly on top of each other (AA stacking) form strong chemical bonds when the distance between planes is 0.156 nm. Simultaneously, C–C in-plane bonds are considerably weakened from partial double bond (0.141 nm) to single bond (0.154 nm). This polymorphic form of graphene bilayer is metastable with an activation energy of 0.16 eV/cell with respect to the standard configuration bound by van der Waals forces at a larger separation between planes (0.335 nm). Carbon atoms form four single bonds in a geometry mixing 90° and 120° angles, intermediate between the usual sp^2 and sp^3 , but similar to the one found in molecules like the cubane, pentaprismane, or hexaprismane. Under an in-plane stress of 9 GPa, this carbon allotrope becomes the global energy minimum. As a function of the separation between layers, the electronic band structure goes through different regimes: It is a semimetal at van der Waals-like distances, a wide gap semiconductor at covalentlike distances, and in between it displays metallic behavior.

DOI: 10.1103/PhysRevB.77.045403

PACS number(s): 73.22.-f, 61.50.Ah, 73.61.Cw, 81.05.Uw

I. INTRODUCTION

Carbon shows one of the richest chemistry in the Periodic Table and it is often found in allotropic forms. Diamond and graphite have a place in textbooks of solid-state physics. The discovery of fullerenes and nanotubes has raised even more interest in carbon-based materials for their potential applications. Recently, the realization of two-dimensional periodic systems made by the stacking of a few graphene layers (FGLs), going down to the single layer, has attracted further interest as the basis for new electronic devices.¹ Several preparation techniques are currently used giving rise to samples showing important differences,^{1–5} most notably, charge accumulation regions associated with physical corrugation found in freestanding graphene,⁵ new properties induced in the graphene layers by the epitaxial growth on a SiC substrate,⁴ or a modification of the stacking, from Bernal AB phase to AA, found in carbon nanofilms grown from graphite oxide.³ Most recently, the possibility to substrate-induced band gaps in epitaxial FGL, or the development of metallic and/or semiconducting properties in bilayers under stress, has increased hopes of finding useful applications for these systems.⁶ Theoretical work that mimics the experimental search for better, new, or more convenient samples has led us to find another type of graphene bilayer that is substantially different from present forms of FGL both because of the type of chemical bonding involved and its characteristic semiconducting electronic band structure. State-of-the-art theoretical total-energy methods show how strong covalent bonds form between graphene layers stacked directly on top of each other (AA) at a distance that is less than half the typical one for an alternating (AB) stacking based on weak van der Waals forces (~ 0.335 nm). On this metastable polymorphic form of a graphene bilayer, each carbon is bonded to the four nearest neighbors, at 0.154 and 0.156 nm for in-plane and out-of-plane bonds, respectively (Fig. 1). Due to the fact that all electrons are allocated in covalent bonds, the bilayer becomes a wide gap semiconductor (indirect gap of 0.91 eV). Intermediate structures between these two limiting cases can be stabilized by external forces. As a function of

the separation between layers, transport properties of the undoped AA stacking are rich: At large distances between planes (e.g., as found in conventional FGL samples), the system is very close to a semimetal, mostly dominated by the single graphene layer properties. As the distance between layers decreases, the bilayer becomes a good metal.

II. THEORETICAL METHODS

Our results are based on *ab initio* calculations taking advantage of density functional theory (DFT).⁷ Exchange and correlation have been computed within a local approximation (LDA).⁸ Including gradient corrections to improve the description of the exchange and correlation functional⁹ (GGA) does not qualitatively change our conclusions; it merely modifies the fine details (GGA overestimates bonding distances by a similar amount as LDA underestimates them and increases the stability of the polymorph by predicting a 26% increase in the barrier). Therefore, LDA has been preferred as a simpler formalism affording a simpler physical

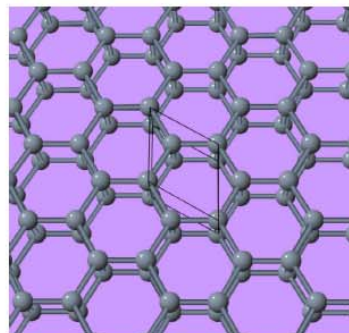


FIG. 1. (Color online) Metastable extended 2D carbon allotrope formed by two graphene layers at covalent C–C bond distance and direct on-top stacking (AA). The 2D unit cell is shown ($a=b=0.267$ nm, $\gamma=120^\circ$).

Stress and Chemical Activity on Graphene

P.L. de Andres¹ and J.A. Vergés¹

¹ *Instituto de Ciencia de Materiales de Madrid
(CSIC) E-28049 Cantoblanco, Madrid (SPAIN)*

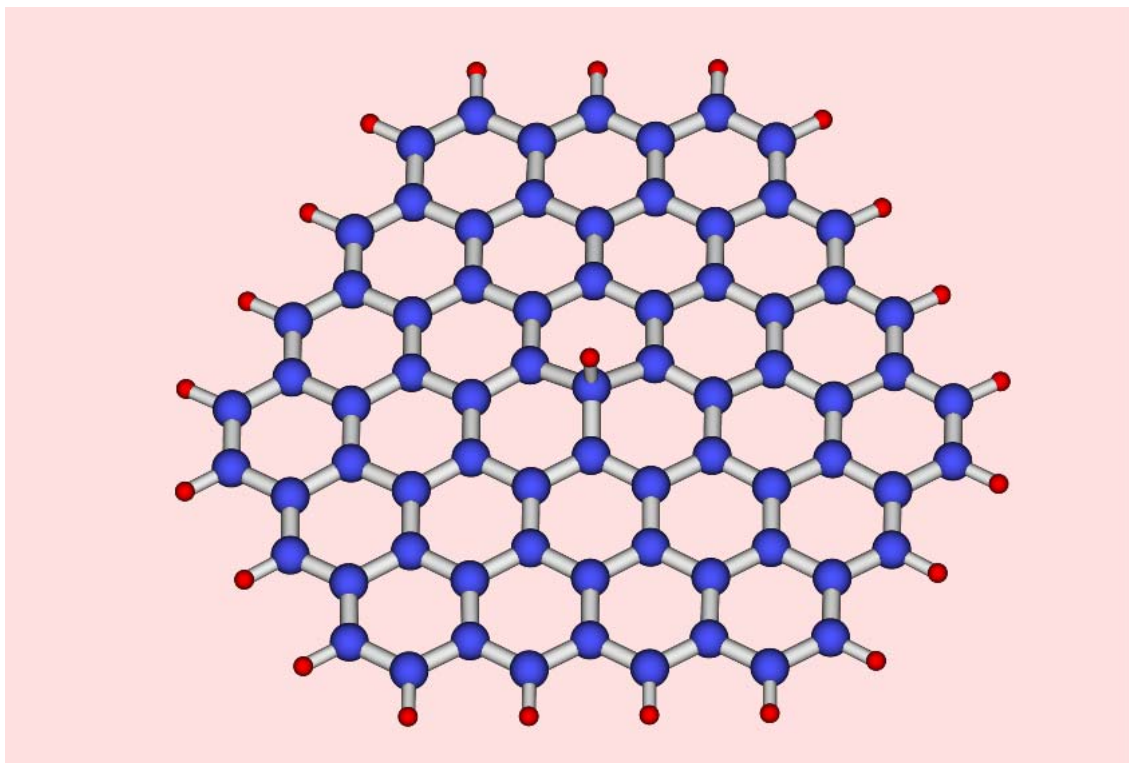
(Dated: June 26, 2008)

Abstract

Graphene layers are stable, hard, and relatively inert, which can be traced to the formation of localized σ bonds and extended π bonds. We study how tensile stress affects these bonds and the resulting change in the chemical activity of a single graphene layer. Stress affects first to the π bonds because it is very effective decoupling the neighbouring p_z orbitals. Electrons on these orbitals become chemically active and can bind to adsorbed species more strongly. Reciprocally, adsorption of chemical species induces significant strains/stresses in the graphene layer. Upon stretch, the 120° in-plane only bonds develop a new character that allows geometries mixing 120° and 90° ; a precursor for the formation of single tetrahedral sp^3 bonds. To illustrate these ideas we simulate from first-principles (Density Functional Theory) the adsorption of a simple atom (hydrogen) and a complex molecule (benzene) on large clusters of carbon and 2D periodic models for graphene.

PACS numbers: 82.45.Jn,68.43.Bc,81.05.Uw,68.35.Gy

Keywords: carbon, graphene, stress, chemical activity, hydrogen, benzene



Water Dimer Diffusion on Pd{111} Assisted by an H-Bond Donor-Acceptor Tunneling ExchangeV. A. Ranea,^{1,*} A. Michaelides,² R. Ramírez,¹ P. L. de Andres,¹ J. A. Vergés,¹ and D. A. King²¹*Instituto de Ciencia de Materiales, Consejo Superior de Investigaciones Científicas, Cantoblanco, E-28049 Madrid, Spain*²*Department of Chemistry, University of Cambridge, Lensfield Road, Cambridge CB2 1EW, United Kingdom*

(Received 3 October 2003; published 2 April 2004)

Based on the results of density functional theory calculations, a novel mechanism for the diffusion of water dimers on metal surfaces is proposed, which relies on the ability of H bonds to rearrange through quantum tunneling. The mechanism involves quasifree rotation of the dimer and exchange of H-bond donor and acceptor molecules. At appropriate temperatures, water dimers diffuse more rapidly than water monomers, thus providing a physical explanation for the experimentally measured high diffusivity of water dimers on Pd{111} [Mitsui *et al.*, *Science* **297**, 1850 (2002)].

DOI: 10.1103/PhysRevLett.92.136104

PACS numbers: 68.43.Bc, 68.43.Fg, 68.43.Jk, 68.47.De

A detailed knowledge of the interaction of water with metal surfaces is important to a great number of fields of scientific endeavor, e.g., electrochemistry, heterogeneous catalysis, and energy production. Recently, in an elegant scanning tunneling microscopy (STM) experiment, Mitsui *et al.* directly tracked the motion of individual water monomers and small water clusters on Pd{111} [1]. Diffusion rates for each of the water fragments were determined. A most striking finding was that at 40 K water dimers diffuse $\approx 10^4$ times faster than the other water clusters. This is an important and intriguing experimental observation that needs to be understood. Mitsui *et al.* suggested that the mismatch between the O-O distance in the dimer (2.95 Å in the gas phase) and the Pd-Pd distance (2.75 Å) of the substrate would destabilize the dimer sufficiently to make its diffusion rapid. Density functional theory (DFT) calculations presented here, however, reveal that there is a much more subtle and widely applicable basis for the rapid diffusion of water dimers. It is not directly related to the mismatch between the adsorbate and substrate, rather the origin is in the H-bonding dynamics of the dimer. Because of the H bond, the adsorbed water dimer is asymmetric: the water donating the H bond (**D**) adsorbs 0.5 Å closer to the surface than the water accepting the H bond (**A**) [Fig. 1(a)]. Indeed, **A** is located at 2.90 Å above the surface and is essentially free to rotate around the low lying **D** molecule to which it is tethered [Figs. 1(a) and 1(b)]. This, coupled with the fact that the four hydrogens in the dimer can exchange positions through tunneling, means that the donor and acceptor roles of the water molecules are readily switched [Figs. 1(b)–1(f)]: **A-D** \leftrightarrow **D-A**. Following this exchange, the heights of **A** and **D** above the surface change according to their new roles, and the dimer is thus free to rotate around a new axis centered at the old **A**. The result of this “molecular waltz” is a net translation of the dimer by a surface lattice spacing. Measurements on the gas phase for the splitting associated to the donor-acceptor exchange by tunneling have been performed

with vibration-rotation-tunneling (VRT) spectroscopy [2] and have been accurately reproduced by calculations that solve the Schrödinger equation in the full six-dimensional intermolecular potential surface [3]. Based on our *ab initio* calculation for water on Pd{111}, we show that this interchange allows water dimers to diffuse more rapidly than monomers below 50 K. We conclude that the unexpectedly high diffusion rate of water dimers on Pd{111} demonstrates how H-bonding interactions can assist adsorbate diffusion and is another example of tunneling at low temperatures between nearby minima on a potential energy surface (PES).

The computational approach used here is based on accurate quantum-mechanical calculations within the DFT formalism. The majority of the calculations are performed in periodically repeating supercells [4], which is most appropriate for studying extended systems like the Pd{111} surface. Core electrons are described through ultrasoft pseudopotentials [5] and the kinetic energy cut-off of the plane-waves basis set is 340 eV. The Perdew-Wang 1991 [6] generalized gradient approximation (GGA) is used throughout. The system is described with a $3 \times 3 \times 3$ supercell and a slab of six layers of Pd. A $3 \times 3 \times 1$ *k*-point mesh has been used [7]. A given configuration is considered converged when the total energy change per atom is less than 2×10^{-5} eV, the root-mean-square (rms) displacement of the nuclei is less than 10^{-3} Å, and the rms force on the atomic nuclei is less than 0.05 eV/Å. Owing to the localized nature of the water-substrate interaction [8,9], water monomer and dimer adsorption were also explored on clusters of 10 to 15 Pd atoms. DFT, as implemented in the GAUSSIAN-98 package [10], was used. A correlation consistent polarized triple zeta basis set was employed for H and O and a Stuttgart/Dresden electron core potential basis set for Pd. The Becke-3-Lee-Yang-Parr (GGA) functional was used for the cluster calculations, which were converged to the Gaussian default thresholds. Despite the clear differences between the slab and cluster calculations, adsorption

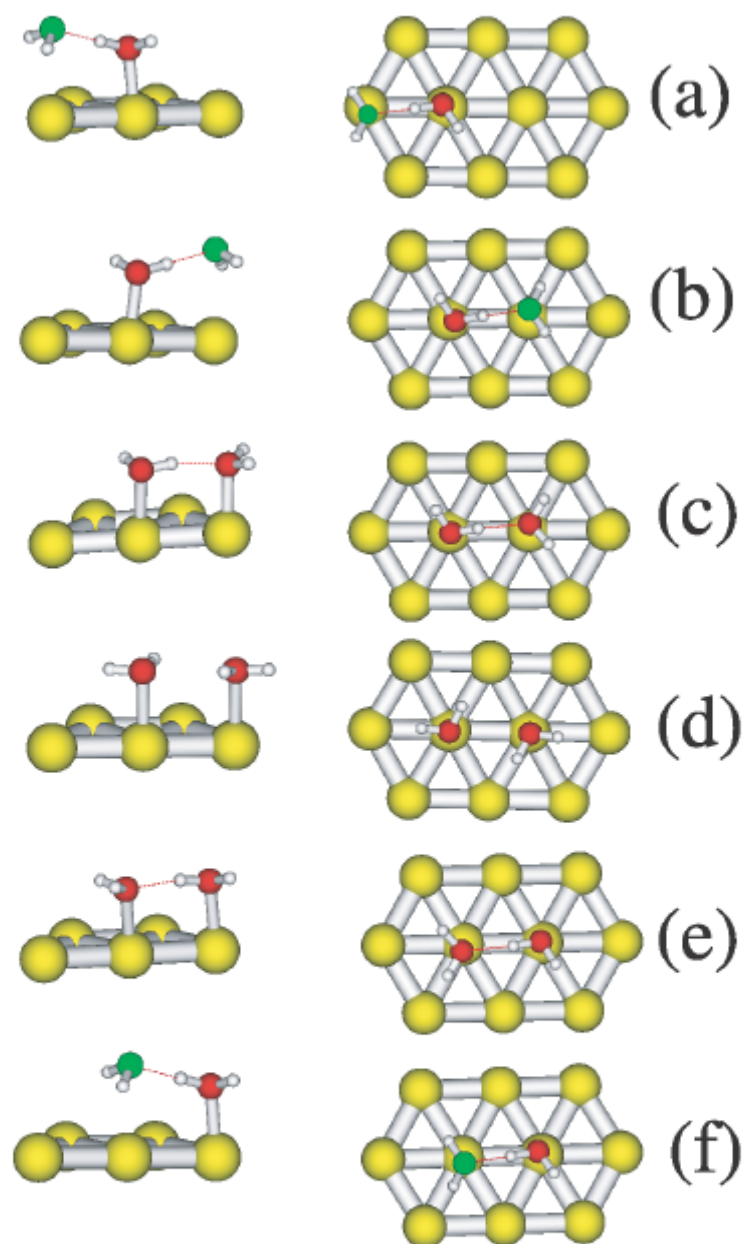


FIG. 1 (color online). Mechanism for water dimer diffusion on Pd{111} (top and side view). Step (a) to (b) involves a nearly free rotation of the dimer; step (b) to (c) is the wagging motion of the dimer, which brings both water molecules to a similar height above the surface from where they can undergo donor-acceptor tunneling interchange (c)-(e). From step (e) to (f), the dimer restores its equilibrium geometry having translated one lattice spacing [compare (a) and (f)].

Hydrogen in α -iron: stress and diffusion

J. Sanchez,¹ J. Fulla,¹ C. Andrade,¹ and P.L. de Andres²

¹ *Instituto de Ciencias de la Construcción,*

"Eduardo Torroja" (CSIC) c/ Serrano Galvache 4, E-28033 Madrid (SPAIN)

² *Instituto de Ciencia de Materiales de Madrid*

(CSIC) E-28049 Cantoblanco, Madrid (SPAIN)

(Dated: June 19, 2008)

Abstract

First-principles density-functional theory has been used to investigate equilibrium geometries, total energies, and diffusion barriers for H as an interstitial impurity absorbed in α -Fe. Internal strains/stresses upon hydrogen absorption are a crucial factor to understand preferred absorption sites and diffusion. For high concentrations, H absorbs near the octahedral site favoring a large tetragonal distortion of the BCC lattice. For low concentration, H absorbs near the tetrahedral site minimizing the elastic energy stored on nearby cells. Diffusion paths depend on the concentration regime too; hydrogen diffuses about ten times faster in the distorted BCT lattice. External stresses of several GPa modify barriers by $\approx 10\%$, and diffusion rates by $\approx 30\%$.

PACS numbers: 66.30.J-,68.43.Bc,71.15.Mb

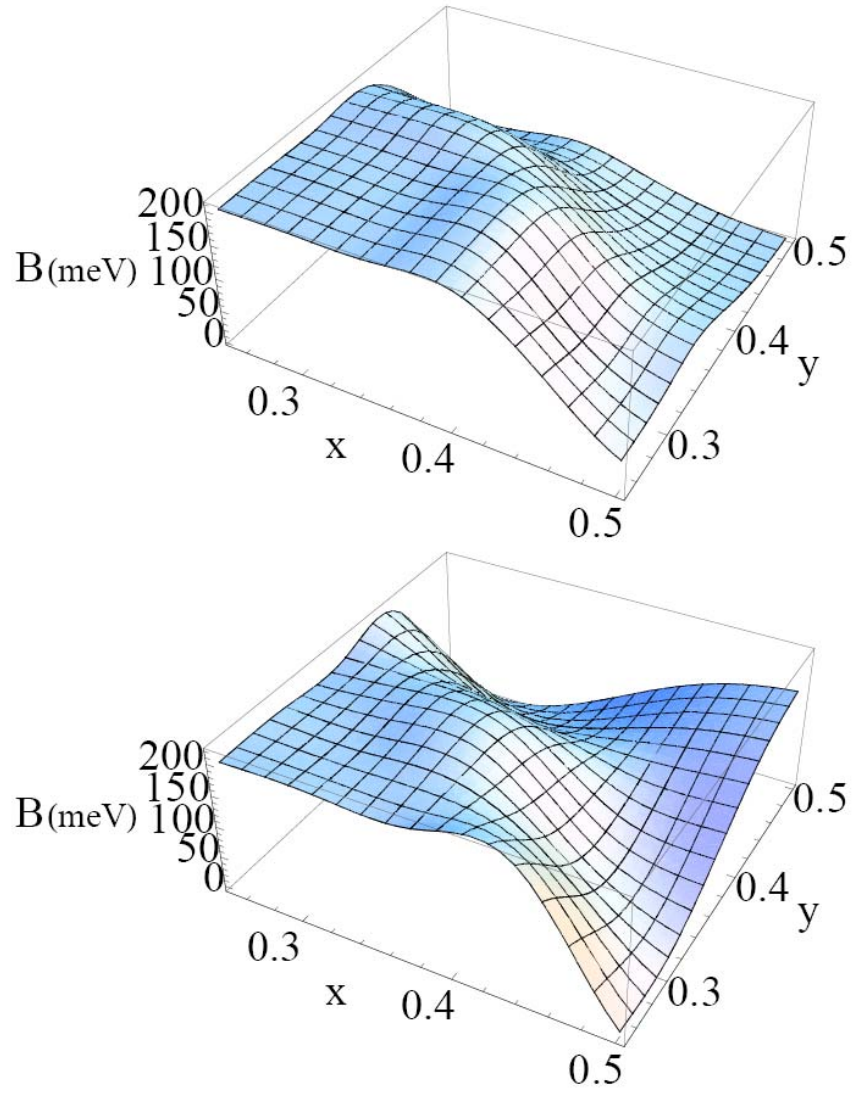


FIG. 3: Total energy (meV) landscapes for (a) high and (b) low concentrations cases (top and bottom panels). x and y are given in fractional units with respect to the $1 \times 1 \times 1$ BCC unit cell. O-site is located at the top right corner $\{\frac{1}{2}, \frac{1}{2}, 0\}$, and T-site at the down right and top left corners. $\{\frac{1}{4}, \frac{1}{2}, 0\}$. The region around the Fe at the origin (higher values than 200 meV) has been artificially put to a constant value to improve visibility of the relevant paths from O-site to T-site (a) and from T-site to T-site (b).

Multiscale modeling of Schottky-barrier MOSFETs with disilicide source/drain contacts: Role of contacts in the carrier injection

M. Dubois,^{1,*} D. Jiménez,² P. L. de Andres,³ and S. Roche¹¹CEA-DRFMC/SPSMS/GT, 17 rue des Martyrs, 38054 Grenoble Cedex 09, France²Departament d'Enginyeria Electrònica, Escola Tècnica Superior d'Enginyeria, Universitat Autònoma de Barcelona, 08193 Bellaterra, Spain³Instituto de Ciencia de Materiales (CSIC), Cantoblanco, E-28049 Madrid, Spain

(Received 12 March 2007; revised manuscript received 21 May 2007; published 28 September 2007)

We report on a multiscale approach for the simulation of electrical characteristics of metal disilicide based Schottky-barrier metal oxide semiconductor field-effect transistors (SB-MOSFETs). Atomistic tight-binding method and nonequilibrium Green's function formalism are combined to calculate the propagation of charge carriers in the metal and the charge distribution at the $MSi_2(111)/Si(111)$ and $MSi_2(111)/Si(100)$ (with $M = Ni, Co, \text{ and } Fe$) contacts. Quantum transmission coefficients at the interfaces are then computed accounting for energy and momentum conservation, and are further used as input parameters for a compact model of SB-MOSFET current-voltage simulations. In the quest for nanodevice performance optimization, this approach allows unveiling the role of different materials in configurations relevant for heterostructure nanowires.

DOI: 10.1103/PhysRevB.76.115337

PACS number(s): 73.40.-c, 85.35.-p, 73.63.-b, 73.30.+y

I. INTRODUCTION

Scaling down metal oxide semiconductor field-effect transistors (MOSFETs) is one of the most challenging tasks for nanoelectronics device designers. As the physical limits of conventional MOSFETs are being reached, alternative structures are proposed to circumvent or limit parasitic effects that emerge with size reduction, such as increasingly large contact resistances owing to intrusive dopant redistribution at the contact/channel interfaces. Among these candidates, Schottky-barrier MOSFETs (SB-MOSFETs) have been widely investigated in recent years, both experimentally¹ and theoretically.²⁻⁴ In SB-MOSFETs, the highly doped source and drain contacts are replaced by metallic ones, which could reduce, in principle, both contact resistances and short channel effects.^{5,6} However, in contrast with the Ohmic contact generally achieved with traditional MOSFETs, SB-MOSFET current-voltage characteristics become largely dominated by the interface electrostatics due to Fermi level pinning.⁷ In the past, this phenomenon has been a major drawback to engineering performant, versatile and well controlled transistor devices and logic circuits.^{8,9}

Despite this situation, remarkable improvements have been achieved in the past years in the epitaxial growth of high quality $NiSi_2$ and $CoSi_2$ films on both (100)- and (111)-oriented silicon substrates, owing to the very similar crystal structures of disilicides and silicon materials.¹⁰ More recently, a metallic phase has been identified for iron disilicide (γ - $FeSi_2$) with the same fluorite structure although its growth on silicon substrates remains delicate.^{11,12} The low Schottky-barrier height (SBH) arising at the interface between these three disilicides and silicon^{13,14} makes them promising materials for the fabrication of metal disilicide source/drain SB-MOSFETs with good performances.

Moreover, catalytically grown undoped silicon nanowires (Si-NWs) have been recently made with a further self-aligned formation of nickel silicide ($NiSi_2$) source and drain segments along the nanowire.^{15,16} The initial characterization

of these nanodevices shows promising performances, such as large sustained current densities.¹⁶ This opens novel perspectives for large scale integration of low-dimensional SB-MOSFETs using chemically driven bottom-up integration methods.

Finally, first principles calculations¹⁷ suggest that weak doping of the silicon channel could strongly reduce the SBH, bringing silicide/silicon contact resistance way below the targeted value of the International Technology Roadmap for Semiconductors.

Schottky contact resistances between disilicides and silicon-based materials are known, however, to be sensitive to quantum reflection phenomena. These backscattering effects occur during charge transfer at the interface because symmetry-induced selection rules of contacted materials restrict the possibilities to simultaneously conserve energy and momentum.¹⁸ It is, thus, of relevance to explore in depth the material-dependent role played by quantum reflections in order to assess the conditions for the ultimate performances of SB-MOSFETs.

In this work, we present a multiscale modeling of SB-MOSFETs with metal disilicide source and drain contacts, combining atomistic based transport calculations with compact modeling of SB-MOSFET devices. The paper is divided as follows. In Sec. II, the atomistic tight-binding Green's function formalism is detailed, and the ballistic propagation of electrons in the metallic source/drain is computed in Sec. III, taking into account the materials' nature, electronic structure, and symmetry orientations. Quantum reflection phenomena are then addressed in Sec. IV by matching the energy and k_{\parallel} vector between outgoing states from the metal and the incoming states in the silicon channel, which is tackled within the effective mass approximation. This allows extracting a transmission coefficient that will be further incorporated into a compact model for the simulation of transistor current-voltage characteristics in a heterostructure nanowire configuration. The theoretical background for this compact model is presented in Sec. V. In this way, we can include

Surface atomic structure determination of three-dimensional yttrium silicide epitaxially grown on Si(111)

C. Rogero, P. L. de Andres, and J. A. Martín-Gago
Instituto Ciencia de Materiales de Madrid-CSIC, 28049-Cantoblanco, Spain
 (Received 14 June 2004; published 11 April 2005)

The surface atomic structure of thin layers of three-dimensional yttrium silicide epitaxially grown on Si(111) 7×7 has been investigated by means of dynamical low-energy electron diffraction analysis. We determine the interlayer distances as well as the lateral and/or vertical relaxations of the atoms in the superficial planes. The epitaxial silicide consists of stacked hexagonal rare-earth planes and graphitelike Si planes with an ordered arrangement of Si vacancies. The ordered net of Si vacancies in the inner planes is responsible for the lateral relaxations of the surrounding Si atoms. The topmost layer does not present a graphitelike structure, forming a buckled Si layer with no vacancies. One of the three Si atoms in the lower plane of this bilayer is closer to the yttrium layer due to the presence of the vacancy in the last Si plane just below. This produces vertical relaxation in the termination layer.

DOI: 10.1103/PhysRevB.71.165306

PACS number(s): 61.14.Hg, 82.45.Mp, 68.35.-p, 68.55.-a

I. INTRODUCTION

Heavy rare-earth (RE) silicides epitaxially grown on *n*-type Si(111) can be used in electronic devices (e.g., infrared detectors, ohmic contacts or rectifying contacts) because of their unusual low values for the Schottky barrier height,¹⁻⁵ and very small lattice mismatch at the interface.⁶⁻⁹ Moreover, the abruptness of the silicide/vacuum interface makes them good candidates to grow new layers on top, offering new perspectives for integrated silicon technology.¹⁰ However, despite their technological relevance an important issue remains open: which is the atomic structure of these silicide surfaces? In this paper we perform a detailed surface structural study for the yttrium silicide by means of dynamical low-energy electron diffraction (LEED).

For thin RE silicides epitaxially grown on Si(111) several surface reconstructions have been reported for different coverages. If less than 1 monolayer (ML) is deposited, different reconstructions are visible, $(2\sqrt{3} \times 2\sqrt{3})R30^\circ$ or (5×5) .¹¹ For RE coverage of around 1 ML, these silicides present a two-dimensional (2D) metallic structure, exhibiting a $p(1 \times 1)$ periodicity.¹² At higher coverage, a $(\sqrt{3} \times \sqrt{3})R30^\circ$ LEED pattern appears, and a three-dimensional (3D) metallic silicide is formed.¹³⁻¹⁹

The atomic structure of the inner silicide planes of these 3D metallic RE silicides grown on Si(111) is sketched in Fig. 1 (we will refer to that as the bulk structure in the present work). It consists of a hexagonal structure derived from the AlB_2 -type geometry: graphitelike Si planes intercalated with RE planes. The Si planes contain vacancies, forming an ordered $(\sqrt{3} \times \sqrt{3})R30^\circ$ network that leads to a $RESi_{1.7}$ stoichiometry (in Fig. 1 Si vacancies are marked as stars).^{14,15} Vacancies play an important role in the atomic and electronic structure of these silicides,²⁰ they release the compressive strain caused by the absence of buckling in the Si planes.²¹ If $c=4.14 \text{ \AA}$ is the distance between two Si planes (or between two RE planes) in the direction perpendicular to the surface, the crystal periodicity is $2c$ (upper panel of Fig. 1). Therefore, the geometry varies for two contiguous silicon planes

due to the position of the Si vacancies. The next Si plane just below or just above of a referenced one has the same $(\sqrt{3} \times \sqrt{3})R30^\circ$ superstructure formed by the vacancies, but it is rotated around the surface normal. *Ab initio* theoretical calculations²² have demonstrated that it is possible to obtain similar total-energy values using different periodicities in the z directions. Lattice parameters of c , $2c$ and even $3c$ have been found compatible with the calculations.²² Similarly, a discrepancy exists in the value of the rotation of the vacancies around the surface normal. Although the most accepted model includes a rotation angle of 120° ,^{15,23} other angular values, like 60° , or 0° , have been published too.²¹

In the last years, theoretical^{22,24,25} and experimental studies^{16,21,26-29} have been carried out in order to determine the surface atomic positions in $RESi_{1.7}$ epitaxially grown on

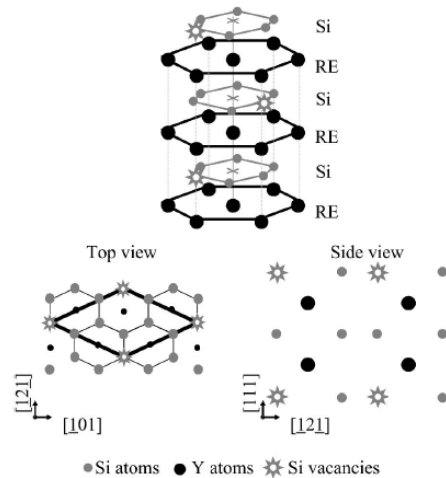
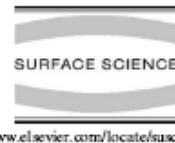


FIG. 1. Schematic representation of the bulk atomic structure of $YSi_{1.7}$. The Si vacancies form a $(\sqrt{3} \times \sqrt{3})R30^\circ$ superstructure.



Surface diffraction structure determination from combinatorial simultaneous optimization

M. Blanco-Rey^{*}, Pedro L. de Andres*Instituto de Ciencia de Materiales (CSIC), Cantoblanco, E-28049 Madrid, Spain*Received 15 December 2005; accepted for publication 31 January 2006
Available online 20 February 2006

Abstract

We present a technique to efficiently locate the global minimum of a cost function on a complex multi-dimensional parameter space (e.g. a structural reliability R -factor). The method builds a convergent series of structures from combinatorial simultaneous optimization of all the parameters on different subspaces of the experimental data base. Performance has been tested for two model situations: (1) phase retrieval from electron scattering by a single atom and (2) low-energy electron diffraction analysis of simulated $I(V)$ curves for the $\text{Ir}(110)\text{-p}(2 \times 1)$ missing row. Compared under the same conditions, a reduction in the computation effort, is found w.r.t. previous state-of-the-art methods (e.g., simulated annealing and genetic algorithms).
© 2006 Elsevier B.V. All rights reserved.

Keywords: Electron-solid diffraction; Low energy electron diffraction (LEED); Surface structure

To understand physical and chemical processes on surfaces a detailed knowledge of atomic positions and/or atomic trajectories is required. A popular way to obtain this information is the analysis of diffraction spectra from different techniques such as low-energy electron diffraction (LEED), photoelectron diffraction (PD), surface X-ray diffraction (SXRD), near-edge X-ray absorption fine structure (NEXAFS), etc. [1–4]. This is a typical inverse problem where the data base, \mathcal{S} , is a function of the structure, \mathcal{X} : $\mathcal{S} = f(\mathcal{X})$. Formally, the problem could be solved by inverting the algorithm relating the structure and the experimental data base $\mathcal{X} = f^{-1}(\mathcal{S})$. In practice, basic problems forbid such a simple procedure, as the lack of information on the phase of the diffracted waves, or the requirement of self-consistency. Therefore, it has been necessary to apply a trial and error procedure that compares experimental and calculated spectra for different proposed models. The quality of the fit for each trial structure is measured by a reliability R -factor, playing the role of a cost

function that must be minimized. The R -factor, as a function of a given structure described by a set of N parameters often displays a complex topography where the global minimum is difficult to locate.

We analyze how to build up an optimum strategy in the context of two problems central to scattering theory: phase-retrieval, and multiple scattering, which are considered the two basic difficulties for direct methods. The simple case of electron scattering by a single atom illustrates the implications of the lack of information on diffracted wave phases [5]. Given an incident plane wave of momentum κ , the scattered amplitude in the far field as a function of the polar angle θ is

$$A(\theta; \kappa) = \frac{1}{2i\kappa} \sum_l (e^{2i\delta_l(\kappa)} - 1) P_l(\cos \theta) \quad (1)$$

where $P_l(\cos \theta)$ are Legendre polynomials. If the phase could be measured, the atomic phase-shifts $\mathbf{x} = \{\delta_l(\kappa)\}$ would be found from Legendre polynomials orthonormal properties. As experiments can only provide the intensities, $I = |A|^2$, we could retrieve the \mathbf{x} by minimizing a cost function such as

^{*} Corresponding author. Fax: +34 91 3720623.
E-mail addresses: maria.blanco@icmm.csic.es (M. Blanco-Rey), pedro@icmm.csic.es (P.L. de Andres).



Molecular t-matrices for Low-Energy Electron Diffraction (TMOL v1.1)^{*}

Maria Blanco-Rey, Pedro de Andres^{*}, Georg Held, David A. King

*Instituto de Ciencia de Materiales (CSIC), Cantoblanco, E-28049 Madrid, Spain
Department of Chemistry, University of Cambridge, Cambridge CB2 1EW, UK*

Received 8 March 2004; accepted 5 May 2004

Available online 2 July 2004

Abstract

We describe a FORTRAN-90 program that computes scattering t-matrices for a molecule. These can be used in a Low-Energy Electron Diffraction program to solve the molecular structural problem very efficiently. The intramolecular multiple scattering is computed within a Dyson-like approach, using free space Green propagators in a basis of spherical waves. The advantage of this approach is related to exploiting the chemical identity of the molecule, and to the simplicity to translate and rotate these t-matrices without performing a new multiple-scattering calculation for each configuration. FORTRAN-90 routines for rotating the resulting t-matrices using Wigner matrices are also provided.

Program summary

Title of program: TMOL

Catalogue number: ADUF

Program summary URL: <http://cpc.cs.qub.ac.uk/summaries/ADUF>

Program obtainable from: CPC Program Library, Queen's University of Belfast, N. Ireland.

Computers: Alpha ev6-21264 (700 MHz) and Pentium-IV.

Operating systems: Digital UNIX V5.0 and Linux (Red Hat 8.0).

Programming language: FORTRAN-90/95 (Compaq True64 compiler, and Intel Fortran Compiler 7.0 for Linux).

High-speed storage required for the test run: minimum 64 Mbytes, it can grow to more depending on the system considered.

Disk storage required: None.

No. of bits in a word: 64 and 32.

No. of lines in distributed program, including test data etc.: 5404

No. of bytes in distributed program, including test data etc.: 59 856

Distribution format: tar.gz

^{*} This paper and its associated computer program are available via the Computer Physics Communications homepage on ScienceDirect. (<http://www.sciencedirect.com/science/journal/00104655>).

^{*} Corresponding author.

E-mail address: pedro@icmm.csic.es (P. de Andres).